

# Title

Ashley N Campbell <sup>\*</sup>, Charles Pepe-Ranney <sup>†</sup>, and Daniel H Buckley <sup>†</sup>

<sup>\*</sup>Department of Microbiology, Cornell University, New York, USA, and <sup>†</sup>Department of Crop and Soil Sciences, Cornell University, New York, USA

Submitted to Proceedings of the National Academy of Sciences of the United States of America

## Abstract

We describe a high-resolution approach for identifying microbial contributions to soil C-cycling dynamics using nucleic acid stable isotope probing coupled with next generation sequencing (HR-SIP). We amended series of soil microcosms with a complex mixture of model carbon (C) substrates and inorganic nutrients common to plant biomass. A single C constituent in the C substrate mixture was substituted for its <sup>13</sup>C-labeled equivalent in each microcosm series. Specifically, in separate microcosms we used substituted <sup>13</sup>C-xylose or <sup>13</sup>C-cellulose for their unlabeled equivalents. Xylose and cellulose were chosen to represent labile soluble C and polymeric insoluble C, respectively. Incorporation of <sup>13</sup>C into DNA was measured at 5 time points in a 30 incubation. 16S rRNA gene sequences from CsCl gradient fractions were profiled by 454 pyrosequencing. Incorporation of <sup>13</sup>C from xylose into microcosm DNA was observed at days 1, 3, and 7, while incorporation of <sup>13</sup>C from cellulose was peaked at day 14 and was maintained through day 40. Of over 6,000 OTUs detected, a total of XX and XX unique OTUs assimilated <sup>13</sup>C from xylose and cellulose, respectively. Xylose assimilating OTUs are more abundant in the microbial community than cellulose assimilating OTUs, while cellulose OTUs demonstrate a greater substrate specificity than xylose OTUs.

monolayer | structure | x-ray reflectivity | molecular electronics

Abbreviations: SAM, self-assembled monolayer; OTS, octadecyltrichlorosilane

## Introduction

We have only a rudimentary understanding of carbon flow through soil microbial communities. This deficiency is driven by the staggering complexity of soil microbial food webs and the opacity of these biological systems to current methods for describing microbial metabolism in the environment. Relating community composition to overall soil processes, such as nitrification and denitrification, which are mediated by defined functional groups has been a useful approach. However, carbon-cycling processes have proven more recalcitrant to study due to the wide range of organisms participating in these reactions and our inability to discern diagnostic functional genetic markers.

Excluding plant biomass, there are 2,300 Pg of carbon (C) stored in soils worldwide which accounts for ~80% of the global terrestrial C pool (BATJES, 1996; Amundson, 2001). When organic C from plants reaches soil it is degraded by fungi, archaea, and bacteria. This C is rapidly returned to the atmosphere as CO<sub>2</sub> or remains in the soil as humic substances that can persist up to 2000 years (Yanagita, 1990). The majority of plant biomass C in soil is respired and produces 10 times more CO<sub>2</sub> than anthropogenic emissions on an annual basis (Chapin, 2002). Global changes in atmospheric CO<sub>2</sub>, temperature, and ecosystem nitrogen inputs, are expected to impact primary production and C inputs to soils (Groenigen *et al.*, 2006) but it remains difficult to predict the response of soil processes to anthropogenic change (DAVIDSON *et al.*, 2006). Current climate change models concur on atmospheric and ocean C predictions but not terrestrial (Friedlingstein *et al.*, 2006). These contrasting terrestrial ecosystem model predictions reflect how little is known about soil C cy-

cling dynamics and it has been suggested that inconsistencies in terrestrial modeling could be improved by elucidating the relationship between dissolved organic carbon and microbial communities in soils (Neff and Asner, 2001).

An estimated 80-90% of C cycling in soil is mediated by microorganisms (Nannipieri *et al.*, 2003a; n.d.). Understanding microbial processing of nutrients in soils presents a special challenge due to the heterogeneous nature of soil ecosystems and methods limitations. Soils are biologically, chemically, and physically complex which affects microbial community composition, diversity, and structure (Nannipieri *et al.*, 2003a). Confounding factors such as physical protection/aggregation, moisture content, pH, temperature, frequency and type of land disturbance, soil history, mineralogy, N quality and availability, and litter quality have all been shown to affect the ability of the soil microbial community to access and metabolize C substrates (Sollins *et al.*, 1996; Kalbitz *et al.*, 2000). Further, rates of metabolism are often measured without knowing the identity of the microbial species involved (Nannipieri *et al.*, 2003b) leaving the importance of community membership towards maintaining ecosystem functions unknown (Nannipieri *et al.*, 2003b; Allison and Martiny, 2008; Schimel and Schaeffer, 2012). Litter bag experiments have shown that the community composition of soils can have quantitative and qualitative impacts on the breakdown of plant materials (Schimel, 1995). Reciprocal exchange of litter type and microbial inocula under controlled environmental conditions reveals that differences in community composition can account for 85% of the variation in litter carbon mineralization (Strickland *et al.*, 2009). In addition, assembled communities of cellulose degraders reveal that the composition of the community has significant impacts on the rate of cellulose degradation (Wohl *et al.*, 2004). An important step in understanding soil C cycling dynamics is to identify individual contributions of discrete microorganisms and to investigate the relationship between genetic diversity, community structure, and function (O'Donnell *et al.*, 2002). The vast majority of microorganisms continue to resist cultivation in the laboratory, and even when cultivation is achieved, the traits expressed by a microorganism in culture may not be representative of those expressed when in its natural habitat. Stable-isotope probing (SIP) provides a unique opportunity to link microbial identity to activity and has been utilized to expand our knowledge of a myriad of important biogeochemical processes (Chen and Murrell, 2010). The most successful applications of this technique have identified organisms which mediate processes performed by a narrow set of functional guilds such as methanogens (Lu, 2005). The technique has been less applica-

## Reserved for Publication Footnotes

ble to the study of soil C cycling because of limitations in resolving power as a result of simultaneous labeling of many different organisms in the community. Additionally, molecular applications such as TRFLP, DGGE, and cloning that are frequently used in conjunction with SIP provide insufficient resolution of taxon identity and depth of coverage. We have developed an approach that employs a complex mixture of substrates added to soil at a low concentration relative to soil organic matter pools along with massively parallel DNA sequencing. This greatly expands the ability of nucleic acid SIP to explore complex patterns of C-cycling in microbial communities with increased resolution.

A temporal cascade occurs in natural microbial communities during the plant biomass degradation in which labile C degradation precedes polymeric C (Hu and Bruggen, 1997; Rui *et al.*, 2009). The aim of this study is to track the temporal dynamics of C assimilation through discrete individuals of the soil microbial community to provide greater insight into soil C-cycling. Our experimental approach employs the addition of a soil organic matter (SOM) simulant (a complex mixture of model carbon sources and inorganic nutrients common to plant biomass), where a single C constituent is substituted for its  $^{13}\text{C}$ -labeled equivalent, to soil. Parallel incubations of soils amended with this complex C mixture allows us to test how different C substrates cascade through discrete taxa within the soil microbial community. In this study we use  $^{13}\text{C}$ -xylose and  $^{13}\text{C}$ -cellulose as a proxy for labile and polymeric C, respectively. Using a novel approach we couple nucleic acid stable isotope probing with next generation sequencing (SIP-NGS) to elucidating soil microbial community members responsible for specific C transformations. Amplicon sequencing of 16S rRNA gene fragments from many gradient fractions and multiple gradients make it possible to track C assimilation by hundreds of different taxa. Ultimately we identify discrete microorganisms responsible for the cycling of specific C substrates.

## Results

To observe C use dynamics by the soil microbial community, we conducted a nucleic acid SIP experiment wherein xylose or cellulose carried the isotopic label, and, we assayed SSU rRNA gene content of CsCl gradient fractions using high-throughput DNA sequencing technology. We set up three soil microcosm series. Microcosms in each series were amended with a C substrate mixture that included cellulose and xylose. The C substrate mixture approximated freshly degrading plant biomass. The same substrate mixture was added to microcosms in each series, however, for each series except the control, one substrate was substituted for its  $^{13}\text{C}$  counterpart. In one series cellulose was  $^{13}\text{C}$ -labeled in another xylose was  $^{13}\text{C}$ -labeled and in the control series no substrates were  $^{13}\text{C}$  labeled. Microcosm amendments are shorthand identified in the following figures by the following code: "13CXPS" refers to the amendment with  $^{13}\text{C}$ -xylose (that is  $^{13}\text{C}$  Xylose Plant Simulant), "13CCPS" refers to the  $^{13}\text{C}$ -cellulose amendment and "12CCPS" refers to the amendment that only contained  $^{12}\text{C}$  substrates. Xylose or cellulose were chosen to carry the isotopic label to contrast C assimilation for labile, soluble C (xylose) versus insoluble, polymeric C (cellulose). 5.3 mg of C substrate mixture per gram soil was added to each microcosm representing 18% of the total soil C. The mixture included 0.42 mg xylose-C and 0.88 mg cellulose-C g soil $^{-1}$ . Microcosms were harvested at days 1, 3, 7, 14 and 30 during a 30 day incubation.  $^{13}\text{C}$ -xylose assimilation peaked immediately and tapered over the 30 day incubation whereas  $^{13}\text{C}$ -cellulose assimilation peaked at two weeks of (Figure 1).

We sequenced SSU rRNA gene amplicons from a total of 277 CsCl gradient fractions from 14 CsCl gradients and 12 bulk microcosm DNA samples. The SSU rRNA gene data set contained

1,376,008 total sequences. The average number of sequences per sample was 3,816 (sd 3,629) and 265 samples had over 1,000 sequences. We sequenced SSU rRNA gene amplicons from an average of 19.8 fractions per CsCl gradient (sd 0.57). The average density between fractions was 0.0040 g mL $^{-1}$ . The sequencing effort recovered a total of 5,940 OTUs. 2,943 of the total 5,940 OTUs were observed in bulk samples. We observed 33 unique phylum and 340 unique genus annotations.

### Soil microcosm microbial community changes with time.

Changes in the soil microcosm microbial community structure and membership correlated with incubation time (Figure 7B, p-value 0.23,  $R^2$  0.63, Adonis test Anderson (2001)). The  $^{13}\text{C}$  composition of the C-substrate addition did not significantly correlate with soil microcosm community structure and membership (p-value 0.35). Additionally, bulk sample beta diversity was significantly less than gradient fraction beta diversity (p-value 0.003, Anderson *et al.* (2006)). Twenty-nine OTUs significantly changed in relative abundance with time ("BH" adjusted p-value < 0.10, Y Benjamini (1995)). OTUs that significantly increased in relative abundance with time included OTUs in the *Verrucomicrobia*, *Proteobacteria*, *Planctomycetes*, *Cyanobacteria*, *Chloroflexi* and *Acidobacteria*. OTUs that significantly decreased in relative abundance with time included OTUs in the *Proteobacteria*, *Firmicutes*, *Bacteroidetes* and *Actinobacteria* (Figure XX). *Proteobacteria* was the only phylum that had OTUs that significantly increased and OTUs that significantly decreased in abundance with time. If sequences were grouped by taxonomic annotations at the class level, only four classes significantly changed in abundance, *Bacilli* (decreased), *Flavobacteria* (decreased), *Gammaproteobacteria* (decreased) and *Herpetosiphonales* (increased) (Figure XX). Of the 29 OTUs that changed significantly in relative abundance with time, 14 are labeled substrate responders (Figure XX).

**OTUs that assimilated  $^{13}\text{C}$  from xylose.** Isotope incorporation by an OTU is revealed by enrichment of the OTU in heavy CsCl gradient fractions containing  $^{13}\text{C}$  labeled DNA relative to heavy fractions from control gradients containing no  $^{13}\text{C}$  labeled DNA. We refer to OTUs that putatively incorporated  $^{13}\text{C}$  into DNA from an isotopically labeled substrate as a substrate "responder". Within the first 7 days of incubation 63% on average of  $^{13}\text{C}$ -xylose was respired and only an additional 6% more was respired from day 7 to 30. At the end of the 30 day incubation 30% of the  $^{13}\text{C}$  from added xylose remained in the soils. The  $^{13}\text{C}$  remaining in the soil from  $^{13}\text{C}$ -xylose addition was likely stabilized by assimilation into microbial biomass and/or microbial conversion into other forms of organic matter. It is also possible that some  $^{13}\text{C}$ -xylose remains unavailable to microbes due to abiotic interactions in soil (Kalbitz *et al.*, 2000).

At day 1, 84% of  $^{13}\text{C}$ -xylose responsive OTUs belong to *Firmicutes*, 11% to *Proteobacteria* and 5% to *Bacteroidetes*. *Firmicutes* responders decreased from 16 OTUs at day 1 to 1 OTU at day 3 while *Bacteroidetes* responders increased from 1 OTU at day 1 to 12 OTUs at day 3. The remaining day 3 responders are members of the *Proteobacteria* (26%) and the *Verrucomicrobia* (5%). Day 7 responders were 53% *Actinobacteria*, 40% *Proteobacteria*, and 7% *Firmicutes*. The identities of  $^{13}\text{C}$ -xylose responders change with time. The numerically dominant  $^{13}\text{C}$ -xylose responder phylum shifts from *Firmicutes* to *Bacteroidetes* and then to *Actinobacteria* across days 1, 3 and 7 (Figure 2, Figure 3).

All of the  $^{13}\text{C}$ -xylose responders in the *Firmicutes* phylum are closely related (at least 99% sequence identity) to cultured isolates from genera that are known to form endospores (Table 2). Each  $^{13}\text{C}$ -xylose responder is closely related to isolates annotated as members of *Bacillus*, *Paenibacillus* or *Lysinibacillus*. *Bacteroidetes*  $^{13}\text{C}$ -xylose responders are predominantly

closely related to *Flavobacterium* species (5 of 8 total responders) (Table 2). Only one *Bacteroidetes*  $^{13}\text{C}$ -xylose responder is not closely related to a cultured isolate, "OTU.183" (closest LTP BLAST hit, *Chitinophaca* sp., 89.5% sequence identity, Table 2). OTU.183 shares high sequence identity with environmental clones derived from rhizosphere samples (accession AM158371, unpublished) and the skin microbiome (accession JF219881, Kong *et al.* (2012)). Other *Bacteroidetes* responders share high sequence identities with canonical soil genera including *Dyadobacter*, *Solibius* and *Terrimonas*. Six of the 8 *Actinobacteria*  $^{13}\text{C}$ -xylose responders are in the *Micrococcales* order. One  $^{13}\text{C}$ -xylose responding *Actinobacteria* OTU shares 100% sequence identity with *Agromyces ramosus* (Table 2). *A. ramosus* is a known predatory bacterium but is not dependent on a host for growth in culture (Casida, n.d.). It is not possible to determine the specific origin of assimilated  $^{13}\text{C}$  in a DNA-SIP experiment.  $^{13}\text{C}$  can be passed down through trophic levels although heavy isotope representation in C pools targeted by cross-feeders and predators would be diluted with depth into the trophic cascade. It's possible, however, that the  $^{13}\text{C}$  labeled *Agromyces* OTU was assimilating  $^{13}\text{C}$  primarily by predation if the *Agromyces* OTU was selective enough with respect to its prey that it primarily attacked  $^{13}\text{C}$ -xylose assimilating organisms.

**$^{13}\text{C}$ -cellulose incorporating OTUs.** Only 2 and 5 OTUs were found to have incorporated  $^{13}\text{C}$  from  $^{13}\text{C}$ -cellulose at days 3 and 7, respectively. At days 14 and 30, however, 42 and 39 OTUs were found to incorporate  $^{13}\text{C}$  from  $^{13}\text{C}$ -cellulose into biomass. An average 16% of the  $^{13}\text{C}$ -cellulose added was respired within the first 7 days, 38% by day 14, and 60% by day 30. A *Cellvibrio* and *Sandaracinaceae* OTU assimilated  $^{13}\text{C}$  from  $^{13}\text{C}$ -cellulose at day 3. Day 7  $^{13}\text{C}$ -cellulose responders included the same *Cellvibrio* responder as day 3, a *Verrucomicrobia* OTU and three *Chloroflexi* OTUs. 50% of Day 14 responders belong to *Proteobacteria* (66% Alpha-, 19% Gamma-, and 14% Beta-) followed by 17% *Planctomycetes*, 14% *Verrucomicrobia*, 10% *Chloroflexi*, 7% *Actinobacteria* and 2% cyanobacteria. *Bacteroidetes* OTUs begin to incorporate  $^{13}\text{C}$  from cellulose at day 30 (13% of day 30 responders). Other day 30 responding phyla include *Proteobacteria* (30% of day 30 responders; 42% Alpha-, 42% Delta, 8% Gamma-, and 8% Beta-), *Planctomycetes* (20%), *Verrucomicrobia* (20%), *Chloroflexi* (13%) and cyanobacteria (3%). *Proteobacteria*, *Verrucomicrobia*, and *Chloroflexi* had relatively high numbers of responders with strong response across multiple time points (Figure 2).

Other notable  $^{13}\text{C}$ -cellulose responders include a *Bacteroidetes* OTU that shares high sequence identity (99%) to *Sporocytophaga myxococcoides* a known cellulose degrader (Vance *et al.*, 1980), and three *Actinobacteria* OTUs that share high sequence identity (100%) with sequenced cultured isolates. One of the three *Actinobacteria*  $^{13}\text{C}$ -cellulose responders is in the *Streptomyces*, a genus known to possess cellulose degraders, while the other two share high sequence identity to cultured isolates *Allotkutzneria alba* (Tomita *et al.*, 1993; Labeda and Kroppenstedt, 2008) and *Lentzea waywayandensis* (LABEDA and LYONS, 1989; Labeda *et al.*, 2001); neither isolate decomposes cellulose in culture. Nine *Planctomycetes* OTUs responded to  $^{13}\text{C}$ -cellulose but none are within described genera (closest cultured isolate match 91% sequence identity, Table 1) (Figure 4). Interestingly, one  $^{13}\text{C}$ -cellulose responder is annotated as "cyanobacteria". The cyanobacteria phylum annotation is misleading as the OTU is not closely related to any oxygenic phototrophs (closest cultured isolate match *Vampirovibrio chlorellavorus*, 95% sequence identity, Table 1). A sister clade to the oxygenic phototrophs classically annotated as "cyanobacteria" in SSU rRNA gene reference databases but does not possess any known phototrophs has recently been proposed to constitute its own phylum, "Melainabac-

teria" Rienzi *et al.* (2013). Although the phylogenetic position of "Melainabacteria" is debated (Soo *et al.*, 2014). The catalog of metabolic capabilities associated with cyanobacteria (or candidate phyla previously annotated as cyanobacteria) are quickly expanding (Rienzi *et al.*, 2013; Soo *et al.*, 2014). Our findings provide evidence for cellulose degradation within a lineage closely related to but apart from oxygenic phototrophs. Notably, polysaccharide degradation is suggested by an analysis of a "Melainabacteria" genome (Rienzi *et al.*, 2013). Although we highlight  $^{13}\text{C}$ -cellulose responders that share high sequence identity with described genera, most  $^{13}\text{C}$ -cellulose responders uncovered in this experiment are not closely related to cultured isolates (Table 1).

*Verrucomicrobia*, a cosmopolitan soil phylum often found in high abundance (Fierer *et al.*, 2013), are hypothesized to degrade polysaccharides in many environments (Fierer *et al.*, 2013; Herlemann *et al.*, 2013; Chin *et al.*, n.d.). *Verrucomicrobia* comprise 16% of the total  $^{13}\text{C}$ -cellulose responder OTUs detected. 40% of *Verrucomicrobia*  $^{13}\text{C}$ -cellulose responders belong to the uncultured "FukuN18" family originally identified in freshwater lakes (Parveen *et al.*, 2013). The *Verrucomicrobia* OTU with the strongest *Verrucomicrobia* response to  $^{13}\text{C}$ -cellulose shared high sequence identity (97%) with an isolate from Norway tundra soil (Jiang *et al.*, 2011) although growth on cellulose was not assessed for this isolate. Only one other  $^{13}\text{C}$ -cellulose responding verrucomicrobium shared high DNA sequence identity with a sequenced type strain, "OTU.638" (Table 1) with *Roseimicrobium gellanilyticum* (100% sequence identity). *Roseimicrobium gellanilyticum* grows on soluble cellulose (Otsuka *et al.*, 2012). The remaining  $^{13}\text{C}$ -cellulose *Verrucomicrobia* responders did not share high sequence identity with any cultured isolates (maximum sequence identity with any cultured isolate 93%).

*Chloroflexi* are traditionally known for metabolically dynamic lifestyles ranging from anoxygenic phototrophy to organohalide respiration (Hug *et al.*, 2013). Recent studies have focused on *Chloroflexi* roles in C cycling (Goldfarb *et al.*, 2011; Cole *et al.*, 2013; Hug *et al.*, 2013) and several *Chloroflexi* utilize cellulose (Goldfarb *et al.*, 2011; Cole *et al.*, 2013; Hug *et al.*, 2013). Four closely related OTUs in an undescribed *Chloroflexi* lineage (closest matching cultured isolate for all four OTUs: *Herpetosiphon geysericola*, 89% sequence identity, Table 1) responded to  $^{13}\text{C}$ -cellulose (Figure 4). One additional OTU also from a poorly characterized *Chloroflexi* lineage (closest cultured isolate match a proteobacterium at 78% sequence identity) responded to  $^{13}\text{C}$ -cellulose (Figure 4).

*Proteobacteria* represent 46% of all  $^{13}\text{C}$ -cellulose responding OTUs identified. *Cellvibrio* accounted for 3% of all proteobacterial  $^{13}\text{C}$ -cellulose responding OTUs detected. *Cellvibrio* was one of the first identified cellulose degrading bacteria and was originally described by Winogradsky in 1929 who named it for its cellulose degrading abilities (Boone, 2001). All  $^{13}\text{C}$ -cellulose responding *Proteobacteria* share high sequence identity with 16S rRNA genes from sequenced cultured isolates (Table 1) except for "OTU.442" (best cultured isolate match 92% sequence identity in the *Chromomyces* genus, Table 1) and "OTU.663" (best cultured isolate match outside *Proteobacteria* entirely, *Clostridium* genus, 89% sequence identity, Table 1). Some *Proteobacteria* responders share high sequence identity with type strains for genera known to possess cellulose degraders including *Rhizobium*, *Devosia*, *Stenotrophomonas* and *Cellvibrio*. One *Proteobacteria* OTU shares high sequence identity with a *Brevundimonas* cultured isolate. *Brevundimonas* has not previously been identified as a cellulose degrader, but has been shown to degrade cellouronic acid, an oxidized form of cellulose (Tavernier *et al.*, 2008).

**Xylose responders are more abundant members of the soil community than cellulose responders.**  $^{13}\text{C}$ -xylose responders are generally more abundant members based on relative abun-

dance in bulk DNA SSU rRNA gene content than  $^{13}\text{C}$ -cellulose responders (Figure 5, p-value 0.00028). However, both abundant and rare OTUs responded to  $^{13}\text{C}$ -xylose and  $^{13}\text{C}$ -cellulose (Figure 5). For instance, a *Delftia*  $^{13}\text{C}$ -cellulose responder is fairly abundant in the bulk samples ("OTU.5", Table 1). OTU.5 was on average the 13th most abundant OTU in bulk samples. A  $^{13}\text{C}$ -xylose responder ("OTU.1040", Table 2) has a mean relative abundance in bulk samples of  $3.57\text{e}^{-05}$ . Two  $^{13}\text{C}$ -cellulose responders were not found in any bulk samples ("OTU.862" and "OTU.1312", Table 1). Of the 10 most abundant responders 8 are  $^{13}\text{C}$ -xylose responders and 6 of these 8 are consistently among the 10 most abundant OTUs in bulk samples.

Responder abundances summed at phylum level generally increased for  $^{13}\text{C}$ -cellulose (Figure XX) whereas  $^{13}\text{C}$ -xylose responder abundances summed at the phylum level decreased over time for *Firmicutes*, *Bacteroidetes*, *Actinobacteria* and *Proteobacteria* although *Proteobacteria* spiked at day 14 (Figure 8). Bulk abundance trends are roughly consistent with  $^{13}\text{C}$  assimilation activity.

**Cellulose degraders exhibit higher substrate specificity than xylose utilizers.** Cellulose responders exhibited a greater shift in BD than xylose responders in response to isotope incorporation (Figure 5, p-value  $1.86\text{e}^{-06}$ ).  $^{13}\text{C}$ -cellulose responders shifted on average 0.0163 g/mL (sd 0.0094) whereas xylose responders shifted on average 0.0097 (sd 0.0094). For reference, 100%  $^{13}\text{C}$  DNA shifts X.XX g/mL relative to the BD of its  $^{12}\text{C}$  counterpart. DNA BD increases as its ratio of  $^{13}\text{C}$  to  $^{12}\text{C}$  increases. An organism that only assimilates C into DNA from a  $^{13}\text{C}$  isotopically labeled source, will have a greater  $^{13}\text{C}:^{12}\text{C}$  ratio in its DNA than an organism utilizing a mixture of isotopically labeled and unlabeled C sources. Upon labeling, DNA from an organism that incorporates exclusively  $^{13}\text{C}$  will increase in buoyant density more than DNA from an organism that does not exclusively utilize isotopically labeled C. Therefore the magnitude DNA buoyant density shifts indicate substrate specificity given our experimental design as only one substrate was labeled in each amendment. We measured density shift as the change in an OTU's density profile center of mass between corresponding control and labeled gradients. Density shifts, however, should not be evaluated on an individual OTU basis as a small number of density shifts are observed for each OTU and the variance of the density shift metric at the level of individual OTUs is unknown. It is therefore more informative to compare density shifts among substrate responder groups. Further, density shifts are based on relative abundance profiles and would be theoretically muted in comparison to density shifts based on absolute abundance profiles and should be interpreted with this transformation in mind. It should also be noted that there was overlap in observed density shifts between  $^{13}\text{C}$ -cellulose and  $^{13}\text{C}$ -xylose responder groups suggesting that although cellulose degraders are generally more substrate specific than xylose utilizers, some cellulose degraders show less substrate specificity for cellulose than some xylose utilizers for xylose (Figure 5), and, each responder group exhibits a range of substrate specificities (Figure 5).

**Estimated *rrn* gene copy number in substrate responder groups.**  $^{13}\text{C}$ -xylose responder estimated *rrn* gene copy number is inversely related to time of first response (p-value  $2.02\text{e}^{-15}$ , Figure 6). OTUs that first respond at later time points have fewer estimated *rrn* copy number than OTUs that first respond earlier (Figure 6). *rrn* copy number estimation is a recent advance in microbiome science (Kembel *et al.*, 2012) while the relationship of *rrn* copy number per genome with ecological strategy is well established (Klappenbach *et al.*, 2000). Microorganisms with a high *rrn* copy number tend to be fast growers specialized to take advantage of boom-bust environments whereas microorganisms with low *rrn* copy number favor slower growth under lower and more consis-

tent nutrient input (Klappenbach *et al.*, 2000). At the beginning of our incubation, OTUs with estimated high *rrn* copy number or "fast-growers" assimilate xylose into biomass and with time slower growers (lower *rrn* copy number) begin to incorporate  $^{13}\text{C}$  from xylose. Further,  $^{13}\text{C}$ -xylose responders have more estimated rRNA operon copy numbers per genome than  $^{13}\text{C}$ -cellulose responders (p-value  $1.87\text{e}^{-09}$ ) suggesting xylose respiring microbes are generally faster growers than cellulose degraders.

## Discussion

Nucleic-acid SIP coupled to microbiome fingerprinting techniques has progressed from simple proof-of-concept experiments CITE, to pilot studies utilizing non-DNA-sequencing microbial community profiling methods such as DGGE CITE and tRFLP CITE, and currently to large experiments employing multiple labeled substrates and high-throughput amplicon and/or shotgun DNA sequencing (Verastegui *et al.*, 2014). We present a high-resolution nucleic acid SIP (HR-SIP) approach that expands upon classical nucleic acid SIP methods in three dimensions: 1) temporally, we sample isotopically labeled substrate amended microcosms at multiple time points; 2) spatially, we assay more fractions along the CsCl gradients; and 3), bioinformatically, we interrogate taxa at the level of OTU for isotope incorporation employing cutting edge statistics for assessing differential abundance in microbiome datasets.

**Ordination of CsCl gradient fraction OTU profiles can be used to observe fraction-level  $^{13}\text{C}$  assimilation dynamics and membership differences.** Each CsCl gradient fraction possesses a unique composition of SSU rRNA gene phylogenetic types. DNA buoyant density (BD) drives differences in CsCl gradient fraction SSU rRNA gene composition. For instance, lighter DNA is more abundant in fractions at lighter densities so DNA with lower G+C will be found in greater abundance at the light end of the CsCl gradient and vice versa. Duplicate gradients receiving only  $^{12}\text{C}$  DNA with the same bulk or non-fractionated SSU rRNA gene phylogenetic composition would have the same overall profile of SSU rRNA gene phylogenetic types across the density gradient. We fed microcosms identical C substrate mixtures save for the identity of a  $^{13}\text{C}$  labeled substrate, and by design, DNA from all microcosms harvested at a time point will be similar in bulk phylogenetic composition. Therefore, SSU rRNA gene profile differences between gradients harvested at the same time are due to  $^{13}\text{C}$  incorporation into bulk community DNA.  $^{13}\text{C}$ -DNA shifts from its  $^{12}\text{C}$  position towards the heavy end of the density gradient. This causes heavy fractions in gradients that received  $^{13}\text{C}$ -DNA to be different in phylogenetic content than corresponding heavy fractions from gradients that received  $^{12}\text{C}$ -DNA of the same bulk phylogenetic composition.

Ordination of CsCl gradient fraction phylogenetic profiles reveals differences and similarities between gradients. It's clear that microcosms incorporated  $^{13}\text{C}$  from both  $^{13}\text{C}$ -xylose and  $^{13}\text{C}$ -cellulose as gradients from both  $^{13}\text{C}$ -xylose and  $^{13}\text{C}$ -cellulose microcosms differ from corresponding control gradients (Figure 1). These differences from control gradients are focused in the heavy fractions (Figure 1). Analysis of SSU rRNA gene surveys has greatly benefited from utilizing conventional methods for data exploration in ecology such as ordination (Lozupone and Knight, 2008). SSU rRNA gene phylogenetic profiles in CsCl gradient fractions have only recently been surveyed with high-throughput DNA sequencing technology and subsequently explored via ordination (Angel and Conrad, 2013; Verastegui *et al.*, 2014). Ordination of CsCl gradient fraction phylogenetic profiles has revealed the relative influence of buoyant density and soil type on gradient phylogenetic profile variance, however, ordination has not demonstrated isotope incorporation. Demonstrating isotope incorporation requires careful comparisons between control and labeled gradients over the

same buoyant density range. By sequencing CsCl gradient fractions from both control and labeled gradients across the full density gradient with DNA harvested from microcosms at multiple time points, we can observe where in the density gradient  $^{13}\text{C}$  isotope incorporation signal is strongest and when  $^{13}\text{C}$  isotope incorporation begins (Figure 1).  $^{13}\text{C}$  incorporation from xylose and cellulose is most apparent at days 1/3/7 and days 14/30, respectively (Figure 1). Moreover, labeled gradient fraction phylogenetic profiles diverge from controls most dramatically at relatively heavy buoyant densities (Figure 1). Also,  $^{13}\text{C}$ -DNA from  $^{13}\text{C}$ -xylose microcosms is different in phylogenetic composition from  $^{13}\text{C}$ -cellulose microcosm  $^{13}\text{C}$ -DNA indicating that xylose and cellulose were assimilated by different microbial community members (Figure 1). Lastly, ordination indicates organisms that assimilated  $^{13}\text{C}$  from  $^{13}\text{C}$ -xylose changed in phylogenetic type over incubation days 1, 3 and 7 (Figure 1).

#### Cellulose degraders identified from undescribed lineages and cosmopolitan soil taxa for which functional attributes are not established

*Verrucomicrobia* are ubiquitous in soil worldwide (Bergmann *et al.*, 2011). *Verrucomicrobia* can constitute 23% of 16S rRNA gene sequences in high-throughput DNA sequencing surveys of SSU rRNA genes in soil (Bergmann *et al.*, 2011) and have been shown to represent as high as 9.8% of soil 16S rRNA (Buckley and Schmidt, 2001). Many *Verrucomicrobia* cultivars have been established in the last decade Wertz *et al.*, 2011 but only one of the 15 most abundant verrucomicrobial phylotypes in a global soil sample collection shared greater than 93% sequence identity with an isolate (Bergmann *et al.*, 2011). Genomic analyses and physiological profiling of *Verrucomicrobia* isolates have revealed methanotrophy and diazotrophy (Wertz *et al.*, 2011) within *Verrucomicrobia* (CITE and reviewed by Wertz *et al.* (2011)). Notably, the genetic capacity to degrade cellulose and cellulose degradation in culture have been demonstrated in *Verrucomicrobia* (Wertz *et al.*, 2011; Otsuka *et al.*, 2012). Although, we have learned many functional roles of *Verrucomicrobia* in the environment, the function and/or global significance of soil *Verrucomicrobia* in global C-cycling is unknown. For example, only one of the putative verrucomicrobial cellulose degraders identified in this experiment are closely related to named cultivars (OTU.XX, Table 1) and only XX% of all verrucomicrobial OTUs found in this study share at least 97% sequence identity with isolates. Seven of 10  $^{13}\text{C}$ -cellulose responding verrucomicrobial OTUs were classified belonging to the *Spartobacteria* order. *Spartobacteria* order was overwhelmingly the numerically dominant order of *Verrucomicrobia* in SSU rRNA gene surveys of 181 globally distributed soil samples (Bergmann *et al.*, 2011). HR-SIP identifies key players in soil C-cycling and *Verrucomicrobia* lineages particularly *Spartobacteria*, given their ubiquity and abundance in soil as well as their demonstrated incorporation of  $^{13}\text{C}$  from  $^{13}\text{C}$ -cellulose, may be significant players in global soil cellulose respiration.

is XX% abundant in soil samples screen by the Earth Microbiome Project (EMP, CITE) and is found in XX of XX EMP soil samples (XX%) and XX of all XX EMP samples (FIGURE).

*Chloroflexi* Banfield paper

Xylose assimilators change over time. Implications for DNA-SIP. Succession within succession.

Response not consistent across phyla.

**Ecological strategies of xylose and cellulose degrading OTUs in soil.** HR-SIP allows us to assess C substrate specificity and temporal dynamics of  $^{13}\text{C}$ -incorporation. C substrate specificity is assessed by measuring the BD shift of OTU DNA upon  $^{13}\text{C}$  incorporation. OTUs that incorporate more  $^{13}\text{C}$  per unit DNA have greater specificity for the labeled substrate than OTUs that incorporate less  $^{13}\text{C}$  per unit DNA.  $^{13}\text{C}$ -cellulose incorporating OTUs

as a group displayed greater substrate specificity than  $^{13}\text{C}$ -xylose incorporating OTUs. This suggests that polymeric C-degraders tend to be specialists tuned to particular C-substrates such as cellulose or lignin whereas labile C-degraders are generalists able to assimilate C from many different labile sources. Although we observed a succession of  $^{13}\text{C}$ -xylose responders (Figure 2 and 3), there was no discernible difference in substrate specificity between  $^{13}\text{C}$ -xylose responders that first responded at days 1, 3 or 7. There was, however, a strong positive relationship between  $^{13}\text{C}$ -xylose responders that first responded at days 1, 3 or 7 in *rrn* copy number.  $^{13}\text{C}$ -xylose responders that first responded at day 1 had higher estimated *rrn* copy number than responders that first responded at day 3 which had higher *rrn* copy number than responders that first responded at day 1. Therefore, OTUs that grow faster assimilate C from xylose faster intuitively. However, fast growers are replaced with respect to C assimilation from xylose with slower growers as xylose diminishes. There was a succession of xylose degraders with time from fast growing spore-formers to *Bacteroidetes* types and finally *Actinobacteria* in out microcosms. The succession hypothesis of decomposition groups ecological units by substrate CITE, however, our results suggest there is a succession of microbial activity for even a single substrate. Hence, in soil, there is an ecological hierarchy coarsely defined by the ability to assimilate C from labile or polymeric sources but then within the labile substrate degraders there are ecological subunits tuned to specific substrate concentrations.

#### Methods

Additional information on sample collection and analytical methods is provided in SI Materials and Methods.

Twelve soil cores (5 cm diameter x 10 cm depth) were collected from six random sampling locations within an organically managed agricultural field in Penn Yan, New York. Soils were pretreated by sieving (2 mm), homogenizing sieved soil, and pre-incubating 10 g of dry soil weight in flasks for 2 weeks. Soils were amended with a 5.3 mg g soil<sup>-1</sup> carbon mixture; representative of natural concentrations Schneckengerber *et al.*, 2008. Mixture contained 38% cellulose, 23% lignin, 20% xylose, 3% arabinose, 1% galactose, 1% glucose, and 0.5% mannose by mass, with the remaining 13.5% mass composed of an amino acid (in-house made replica of Teknova C0705) and basal salt mixture (Murashige and Skoog, Sigma Aldrich M5524). Three parallel treatments were performed; (1) unlabeled control, (2)  $^{13}\text{C}$ -cellulose, (3)  $^{13}\text{C}$ -xylose (98 atom%  $^{13}\text{C}$ , Sigma Aldrich). Each treatment had 2 replicates per time point (n = 4) except day 30 which had 4 replicates; total microcosms per treatment n = 12, except  $^{13}\text{C}$ -cellulose which was not sampled at day 1, n = 10. Other details relating to substrate addition can be found in SI. Microcosms were sampled destructively (stored at -80°C until nucleic acid processing) at days 1 (control and xylose only), 3, 7, 14, and 30.

Nucleic acids were extracted using a modified Griffiths protocol Griffiths *et al.*, 2000. To prepare nucleic acid extracts for isopycnic centrifugation as previously described Buckley *et al.*, 2007, DNA was size selected (>4kb) using 1% low melt agarose gel and  $\beta$ -agarase I enzyme extraction per manufacturers protocol (New England Biolab, M0392S). For each time point in the series isopycnic gradients were setup using a modified protocol Neufeld *et al.*, 2007 for a total of five  $^{12}\text{C}$ -control, five  $^{13}\text{C}$ -xylose, and four  $^{13}\text{C}$ -cellulose microcosms. A density gradient (average density 1.69 g mL<sup>-1</sup>) solution of 1.762 g cesium chloride (CsCl) mL<sup>-1</sup> in gradient buffer solution (pH 8.0 15 mM Tris-HCl, 15 mM EDTA, 15 mM KCl) was used to separate  $^{13}\text{C}$ -enriched and  $^{12}\text{C}$ -nonenriched DNA. Each gradient was loaded with approximately 5  $\mu\text{g}$  of DNA and ultracentrifuged for 66 h at 55,000 rpm and room temperature (RT). Fractions of ~100  $\mu\text{L}$  were collected from below by displacing the DNA-CsCl-gradient buffer solution in the centrifugation tube with

water using a syringe pump at a flow rate of  $3.3 \mu\text{L s}^{-1}$  Mane-field *et al.*, 2002 into Acroprep™ 96 filter plate (Pall Life Sciences 5035). The refractive index of each fraction was measured using a Reichart AR200 digital refractometer modified as previously described Buckley *et al.*, 2007 to measure a volume of  $5 \mu\text{L}$ . Then buoyant density was calculated from the refractive index as previously described Buckley *et al.*, 2007 (see also SI). The collected DNA fractions were purified by repetitive washing of Acroprep filter wells with TE. Finally,  $50 \mu\text{L}$  TE was added to each fraction then resuspended DNA was pipetted off the filter into a new microfuge tube.

For every gradient, 20 fractions were chosen for sequencing between the density range  $1.67\text{--}1.75 \text{ g mL}^{-1}$ . Barcoded 454 primers were designed using 454-specific adapter B, 10 bp barcodes Hamady *et al.*, 2008, a 2 bp linker (5'-CA-3'), and 806R primer for reverse primer (BA806R); and 454-specific adapter A, a 2 bp linker (5'-TC-3'), and 515F primer for forward primer (BA515F). Each fraction was PCR amplified using  $0.25 \mu\text{L}$   $5 \text{ U } \mu\text{L}^{-1}$  AmpliTaq Gold (Life Technologies, Grand Island, NY; N8080243),  $2.5 \mu\text{L}$  10X Buffer II (100 mM Tris-HCl, pH 8.3, 500 mM KCl),  $2.5 \mu\text{L}$  25 mM  $\text{MgCl}_2$ ,  $4 \mu\text{L}$  5 mM dNTP,  $1.25 \mu\text{L}$  10 mg  $\text{mL}^{-1}$  BSA,  $0.5 \mu\text{L}$  10  $\mu\text{M}$  BA515F,  $1 \mu\text{L}$  5  $\mu\text{M}$  BA806R,  $3 \mu\text{L}$   $\text{H}_2\text{O}$ ,  $10 \mu\text{L}$  1:30 DNA template) in triplicate. Samples were normalized either using Pico green quantification and manual calculation or by SequalPrep™ normalization plates (Invitrogen, Carlsbad, CA; A10510), then pooled in equimolar concentrations. Pooled DNA was gel extracted from a 1% agarose gel using Wizard SV gel and PCR clean-up system (Promega, Madison, WI; A9281) per manufacturer's protocol. Amplicons were sequenced on Roche 454 FLX system using titanium chemistry at Selah Genomics (formerly EnGenCore, Columbia, SC)

## References

- Academic Press.
- Allison, SD, Martiny, JBH. (2008). Resistance resilience, and redundancy in microbial communities. *Proc Natl Acad Sci USA* **105**: 11512–11519.
- Amundson, R. (2001). THE CARBON BUDGET IN SOILS. *Ann Rev Earth Planet Sci* **29**: 535–562.
- Anderson, MJ. (2001). A new method for non-parametric multivariate analysis of variance. *Austral Ecology* **26**: 32–46.
- Anderson, MJ, Ellingsen, KE, McArdle, BH. (2006). Multivariate dispersion as a measure of beta diversity. *Ecology Letters* **9**: 683–693.
- Angel, R, Conrad, R. (2013). Elucidating the microbial resuscitation cascade in biological soil crusts following a simulated rain event. *Environ Microbiol*. n/a–n/a.
- BATJES, N. (1996). Total carbon and nitrogen in the soils of the world. *European Journal of Soil Science* **47**: 151–163.
- Bergmann, GT, Bates, ST, Eilers, KG, Lauber, CL, Caporaso, JG, Walters, WA, *et al.* (2011). The under-recognized dominance of Verrucomicrobia in soil bacterial communities. *Soil Biol Biochem* **43**: 1450–1455.
- Boone, D. (2001). *Bergey's manual of systematic bacteriology*. Springer: New York.
- Buckley, DH, Huangyutham, V, Hsu, SF, Nelson, TA. (2007). Stable Isotope Probing with  $^{15}\text{N}$  Achieved by Disentangling the Effects of Genome G+C Content and Isotope Enrichment on DNA Density. *Appl Environ Microbiol* **73**: 3189–3195.
- Buckley, DH, Schmidt, TM. (2001). Environmental factors influencing the distribution of rRNA from Verrucomicrobia in soil. *FEMS Microbiology Ecology* **35**: 105–112.
- Casida, L. Interaction of *Agromyces ramosus* with Other Bacteria in Soil. *Appl Environ Microbiol* **46**: 881–8.
- Chapin, F. (2002). *Principles of terrestrial ecosystem ecology*. Springer: New York.
- Chen, Y, Murrell, JC. (2010). When metagenomics meets stable-isotope probing: progress and perspectives. *Trends in Microbiology* **18**: 157–163.
- Chin, K, Hahn, D, Hengstmann, U, Liesack, W, Janssen, P. Characterization and identification of numerically abundant culturable bacteria from the anoxic bulk soil of rice paddy microcosms. **65**: 5042–9.
- Cole, JK, Gieler, BA, Heisler, DL, Palisoc, MM, Williams, AJ, Dohnalkova, AC, *et al.* (2013). *Kallotenue papyrolyticum* gen. nov. sp. nov., a cellulolytic and filamentous thermophile that represents a novel lineage (Kallotenuales ord. nov., Kallotenuaceae fam. nov.) within the class Chloroflexia. *INTERNATIONAL JOURNAL OF SYSTEMATIC AND EVOLUTIONARY MICROBIOLOGY* **63**: 4675–4682.
- DAVIDSON, EA, JANSSENS, IA, LUO, Y. (2006). On the variability of respiration in terrestrial ecosystems: moving beyond Q10. *Global Change Biol* **12**: 154–164.
- Fierer, N, Ladau, J, Clemente, JC, Leff, JW, Owens, SM, Pollard, KS, *et al.* (2013). Reconstructing the Microbial Diversity and Function of Pre-Agricultural Tallgrass Prairie Soils in the United States. *Science* **342**: 621–624.
- Friedlingstein, P, Cox, P, Betts, R, Bopp, L, Bloh, W von, Brovkin, V, *et al.* (2006). Climate–Carbon Cycle Feedback Analysis: Results from the C4 MIP Model Intercomparison. *Journal of Climate* **19**: 3337–3353.
- Goldfarb, KC, Karaoz, U, Hanson, CA, Santee, CA, Bradford, MA, Treseder, KK, *et al.* (2011). Differential Growth Responses of Soil Bacterial Taxa to Carbon Substrates of Varying Chemical Recalcitrance. *Frontiers in Microbiology* **2**.
- Griffiths, RI, Whiteley, AS, O'Donnell, AG, Bailey, MJ. (2000). Rapid Method for Coextraction of DNA and RNA from Natural Environments for Analysis of Ribosomal DNA- and rRNA-Based Microbial Community Composition. *Appl Environ Microbiol* **66**: 5488–5491.
- Groenigen, KJ, Graaff, MA, Six, J, Harris, D, Kuikman, P, Kessel, C. (2006). The Impact of Elevated Atmospheric  $[\text{CO}_2]$  on Soil C and N Dynamics: A Meta-Analysis. In: *Managed ecosystems and  $\text{CO}_2$* . Springer Science + Business Media, pp. 373–391.
- Hamady, M, Walker, JJ, Harris, JK, Gold, NJ, Knight, R. (2008). Error-correcting barcoded primers for pyrosequencing hundreds of samples in multiplex. *Nat Meth* **5**: 235–237.
- Herlemann, DPR, Lundin, D, Labrenz, M, Jurgens, K, Zheng, Z, Aspeborg, H, *et al.* (2013). Metagenomic De Novo Assembly of an Aquatic Representative of the Verrucomicrobial Class Spar-tobacteria. *mBio* **4**.
- Hu, S, Bruggen, A van. (1997). Microbial Dynamics Associated with Multiphasic Decomposition of  $^{14}\text{C}$ -Labeled Cellulose in Soil. *Microb Ecol* **33**: 134–143.
- Hug, LA, Castelle, CJ, Wrighton, KC, Thomas, BC, Sharon, I, Frischkorn, KR, *et al.* (2013). Community genomic analyses constrain the distribution of metabolic traits across the Chloroflexi phylum and indicate roles in sediment carbon cycling. *Microbiome* **1**: 22.
- Jiang, F, Li, W, Xiao, M, Dai, J, Kan, W, Chen, L, *et al.* (2011). *Luteolibacter luojiensis* sp. nov. isolated from Arctic tundra soil, and emended description of the genus *Luteolibacter*. *INTERNATIONAL JOURNAL OF SYSTEMATIC AND EVOLUTIONARY MICROBIOLOGY* **62**: 2259–2263.
- Kalbitz, K, Solinger, S, Park, JH, Michalzik, B, Matzner, E. (2000). CONTROLS ON THE DYNAMICS OF DISSOLVED ORGANIC MATTER IN SOILS: A REVIEW. *Soil Science* **165**: 277–304.
- Kemmel, SW, Wu, M, Eisen, JA, Green, JL. (2012). Incorporating 16S Gene Copy Number Information Improves Estimates of Microbial Diversity and Abundance. *PLoS Computational Biology* **8**: ed. by C von Mering. e1002743.

- Klappenbach, JA, Dunbar, JM, Schmidt, TM. (2000). rRNA Operon Copy Number Reflects Ecological Strategies of Bacteria. *Appl Environ Microbiol* **66**: 1328–1333.
- Kong, HH, Oh, J, Deming, C, Conlan, S, Grice, EA, Beatson, MA, et al. (2012). Temporal shifts in the skin microbiome associated with disease flares and treatment in children with atopic dermatitis. *Genome Res* **22**: 850–859.
- Labeda, DP, Hatano, K, Kroppenstedt, RM, Tamura, T. (2001). Revival of the genus *Lentzea* and proposal for *Lechevalieria* gen. nov. *INTERNATIONAL JOURNAL OF SYSTEMATIC AND EVOLUTIONARY MICROBIOLOGY* **51**: 1045–1050.
- Labeda, DP, Kroppenstedt, RM. (2008). Proposal for the new genus *Allokutzneria* gen. nov. within the suborder *Pseudonocardineae* and transfer of *Kibdelosporangium albatum* Tomita et al. 1993 as *Allokutzneria albata* comb. nov. *INTERNATIONAL JOURNAL OF SYSTEMATIC AND EVOLUTIONARY MICROBIOLOGY* **58**: 1472–1475.
- LABEDA, DP, LYONS, AJ. (1989). *Saccharothrix texasensis* sp. nov. and *Saccharothrix waywayandensis* sp. nov. *International Journal of Systematic Bacteriology* **39**: 355–358.
- Lozupone, CA, Knight, R. (2008). Species divergence and the measurement of microbial diversity. *FEMS Microbiology Reviews* **32**: 557–578.
- Lu, Y. (2005). In Situ Stable Isotope Probing of Methanogenic Archaea in the Rice Rhizosphere. *Science* **309**: 1088–1090.
- Manefield, M, Whiteley, AS, Griffiths, RI, Bailey, MJ. (2002). RNA Stable Isotope Probing a Novel Means of Linking Microbial Community Function to Phylogeny. *Appl Environ Microbiol* **68**: 5367–5373.
- Nannipieri, P, Ascher, J, Ceccherini, MT, Landi, L, Pietramellara, G, Renella, G. (2003a). Microbial diversity and soil functions. *European Journal of Soil Science* **54**: 655–670.
- Nannipieri, P, Ascher, J, Ceccherini, MT, Landi, L, Pietramellara, G, Renella, G. (2003b). Microbial diversity and soil functions. *European Journal of Soil Science* **54**: 655–670.
- Neff, JC, Asner, GP. (2001). Dissolved Organic Carbon in Terrestrial Ecosystems: Synthesis and a Model. *Ecosystems* **4**: 29–48.
- Neufeld, JD, Vohra, J, Dumont, MG, Lueders, T, Manefield, M, Friedrich, MW, et al. (2007). DNA stable-isotope probing. *Nat Protoc* **2**: 860–866.
- O'Donnell, AG, Seasman, M, Macrae, A, Waite, I, Davies, JT. (2002). Plants and fertilisers as drivers of change in microbial community structure and function in soils. In: *Interactions in the root environment: an integrated approach*. Springer Netherlands, pp. 135–145.
- Otsuka, S, Ueda, H, Suenaga, T, Uchino, Y, Hamada, M, Yokota, A, et al. (2012). *Roseimicrobium gellanilyticum* gen. nov. sp. nov., a new member of the class *Verrucomicrobiae*. *INTERNATIONAL JOURNAL OF SYSTEMATIC AND EVOLUTIONARY MICROBIOLOGY* **63**: 1982–1986.
- Parveen, B, Mary, I, Vellet, A, Ravet, V, Debroas, D. (2013). Temporal dynamics and phylogenetic diversity of free-living and particle-associated *Verrucomicrobia* communities in relation to environmental variables in a mesotrophic lake. *{FEMS} Microbiol Ecol* **83**: 189–201.
- Rienzi, SCD, Sharon, I, Wrighton, KC, Koren, O, Hug, LA, Thomas, BC, et al. (2013). The human gut and groundwater harbor non-photosynthetic bacteria belonging to a new candidate phylum sibling to *Cyanobacteria*. *eLIFE* **2**:
- Rui, J, Peng, J, Lu, Y. (2009). Succession of Bacterial Populations during Plant Residue Decomposition in Rice Field Soil. *Appl Environ Microbiol* **75**: 4879–4886.
- Schimel, J. (1995). Ecosystem Consequences of Microbial Diversity and Community Structure. In: *Arctic and alpine biodiversity: patterns causes and ecosystem consequences*. Springer Science + Business Media, pp. 239–254.
- Schimel, JP, Schaeffer, SM. (2012). Microbial control over carbon cycling in soil. *Frontiers in Microbiology* **3**:
- Schneckenberger, K, Demin, D, Stahr, K, Kuzyakov, Y. (2008). Microbial utilization and mineralization of [<sup>14</sup>C]glucose added in six orders of concentration to soil. *Soil Biol Biochem* **40**: 1981–1988.
- Sollins, P, Homann, P, Caldwell, BA. (1996). Stabilization and destabilization of soil organic matter: mechanisms and controls. *Geoderma* **74**: 65–105.
- Soo, RM, Skennerton, CT, Sekiguchi, Y, Imelfort, M, Paech, SJ, Dennis, PG, et al. (2014). An Expanded Genomic Representation of the Phylum *Cyanobacteria*. *Genome Biology and Evolution* **6**: 1031–1045.
- Strickland, MS, Lauber, C, Fierer, N, Bradford, MA. (2009). Testing the functional significance of microbial community composition. *Ecology* **90**: 441–451.
- Tavernier, ML, Delattre, C, Petit, E, Michaud, P. (2008).  $\beta$ -(1,4)-Polyglucuronic Acids - An Overview. *{TOBIOTJ}* **2**: 73–86.
- Tomita, K, Hoshino, Y, Miyaki, T. (1993). *Kibdelosporangium albatum* sp. nov. Producer of the Antiviral Antibiotics Cycloviracins. *International Journal of Systematic Bacteriology* **43**: 297–301.
- Vance, I, Topham, CM, Blayden, SL, Tampion, J. (1980). Extracellular Cellulase Production by *Sporocytophaga myxococcoides* NCIB 8639. *Microbiology* **117**: 235–241.
- Verastegui, Y, Cheng, J, Engel, K, Kolczynski, D, Mortimer, S, Lavigne, J, et al. (2014). Multisubstrate Isotope Labeling and Metagenomic Analysis of Active Soil Bacterial Communities. *mBio* **5**:
- Wertz, JT, Kim, E, Breznak, JA, Schmidt, TM, Rodrigues, JLM. (2011). Genomic and Physiological Characterization of the *Verrucomicrobia* Isolate *Diplosphaera colitermitum* gen. nov. sp. nov., Reveals Microaerophily and Nitrogen Fixation Genes. *Appl Environ Microbiol* **78**: 1544–1555.
- Wohl, DL, Arora, S, Gladstone, JR. (2004). FUNCTIONAL REDUNDANCY SUPPORTS BIODIVERSITY AND ECOSYSTEM FUNCTION IN A CLOSED AND CONSTANT ENVIRONMENT. *Ecology* **85**: 1534–1540.
- Y Benjamini, YH. (1995). Controlling the False Discovery Rate: A Practical and Powerful Approach to Multiple Testing. *J. Royal Statist. Soc., Series B* **57**: 289–300.
- Yanagita, T. (1990). Natural microbial communities: ecological and physiological features. Japan Scientific Societies Press. Springer-Verlag.

## Figures

Table 1: <sup>13</sup>C-cellulose responders BLAST against Living Tree Project

OTU ID	Fold change	Top BLAST hits	BLAST %ID	Phylum;Class;Order
OTU.862	5.87	<i>Allokutzneria albata</i>	100.0	Actinobacteria Pseudonocardiales Pseudonocardiaceae
OTU.257	2.94	<i>Lentzea waywayandensis</i> , <i>Lentzea flaviverrucosa</i>	100.0	Actinobacteria Pseudonocardiales Pseudonocardiaceae
OTU.132	2.81	<i>Streptomyces</i> spp.	100.0	Actinobacteria Streptomycetales Streptomycetaceae
OTU.465	3.79	<i>Ohtaekwangia kribbensis</i>	92.73	Bacteroidetes Cytophagia Cytophagales
OTU.1094	3.69	<i>Sporocytophaga myxococcoides</i>	99.55	Bacteroidetes Cytophagia Cytophagales
OTU.669	3.34	<i>Ohtaekwangia koreensis</i>	92.69	Bacteroidetes Cytophagia Cytophagales
OTU.573	3.03	<i>Adhaeribacter aerophilus</i>	92.76	Bacteroidetes Cytophagia Cytophagales
OTU.670	2.87	<i>Adhaeribacter aerophilus</i>	91.78	Bacteroidetes Cytophagia Cytophagales
OTU.971	3.68	No hits of at least 90% identity	78.57	Chloroflexi Anaerolineae Anaerolineales
OTU.64	4.31	No hits of at least 90% identity	89.5	Chloroflexi Herpetosiphonales Herpetosiphonaceae
OTU.4322	4.19	No hits of at least 90% identity	89.14	Chloroflexi Herpetosiphonales Herpetosiphonaceae
OTU.98	3.68	No hits of at least 90% identity	88.18	Chloroflexi Herpetosiphonales Herpetosiphonaceae
OTU.5190	3.6	No hits of at least 90% identity	88.13	Chloroflexi Herpetosiphonales Herpetosiphonaceae
OTU.120	4.76	<i>Vampirovibrio chlorellavorus</i>	94.52	Cyanobacteria SM1D11 uncultured-bacterium
OTU.1065	5.31	No hits of at least 90% identity	84.55	Planctomycetes Planctomycetacia Planctomycetales
OTU.484	4.92	No hits of at least 90% identity	89.09	Planctomycetes Planctomycetacia Planctomycetales
OTU.1204	4.32	<i>Planctomyces limnophilus</i>	91.78	Planctomycetes Planctomycetacia Planctomycetales
OTU.150	4.06	No hits of at least 90% identity	86.76	Planctomycetes Planctomycetacia Planctomycetales
OTU.663	3.63	<i>Pirellula staleyi</i> DSM 6068	90.87	Planctomycetes Planctomycetacia Planctomycetales
OTU.473	3.58	<i>Pirellula staleyi</i> DSM 6068	90.91	Planctomycetes Planctomycetacia Planctomycetales
OTU.285	3.55	<i>Blastopirellula marina</i>	90.87	Planctomycetes Planctomycetacia Planctomycetales
OTU.351	3.54	<i>Pirellula staleyi</i> DSM 6068	91.86	Planctomycetes Planctomycetacia Planctomycetales
OTU.600	3.48	No hits of at least 90% identity	80.37	Planctomycetes Planctomycetacia Planctomycetales
OTU.900	4.87	<i>Brevundimonas vesicularis</i> , <i>Brevundimonas nasdae</i>	100.0	Proteobacteria Alphaproteobacteria Caulobacterales
OTU.1754	4.48	<i>Asticcacaulis biprosthecium</i> , <i>Asticcacaulis benevestitus</i>	96.8	Proteobacteria Alphaproteobacteria Caulobacterales
OTU.119	3.31	<i>Brevundimonas alba</i>	100.0	Proteobacteria Alphaproteobacteria Caulobacterales
OTU.327	2.99	<i>Asticcacaulis biprosthecium</i> , <i>Asticcacaulis benevestitus</i>	98.63	Proteobacteria Alphaproteobacteria Caulobacterales
OTU.982	4.47	<i>Devosia neptuniae</i>	100.0	Proteobacteria Alphaproteobacteria Rhizobiales
OTU.1087	4.32	<i>Devosia soli</i> , <i>Devosia crocina</i> , <i>Devosia riboflavina</i>	99.09	Proteobacteria Alphaproteobacteria Rhizobiales
OTU.5539	4.01	<i>Devosia subaequoris</i>	98.17	Proteobacteria Alphaproteobacteria Rhizobiales
OTU.3775	3.88	<i>Devosia glacialis</i> , <i>Devosia chinhatensis</i> , <i>Devosia geojensis</i> , <i>Devosia yakushimensis</i>	98.63	Proteobacteria Alphaproteobacteria Rhizobiales
OTU.429	3.7	<i>Devosia limi</i> , <i>Devosia psychrophila</i>	97.72	Proteobacteria Alphaproteobacteria Rhizobiales
OTU.766	3.21	<i>Devosia insulae</i>	99.54	Proteobacteria Alphaproteobacteria Rhizobiales
OTU.165	3.1	<i>Rhizobium</i> spp.	100.0	Proteobacteria Alphaproteobacteria Rhizobiales



Table 1 – continued from previous page

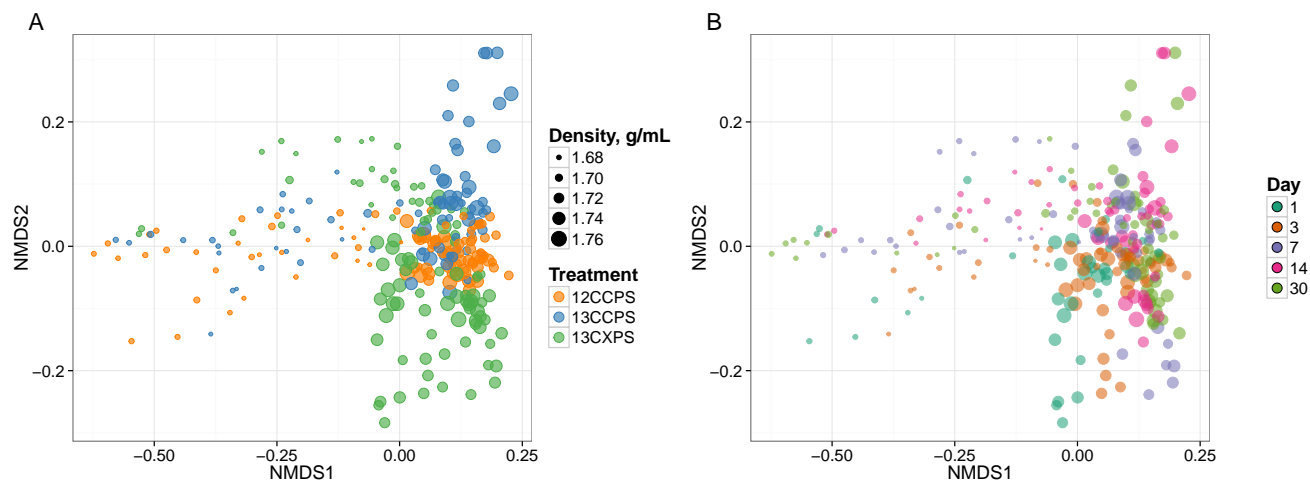
OTU ID	Fold change	Top BLAST hits	BLAST %ID	Phylum;Class;Order
OTU.28	2.59	<i>Rhizobium giardinii</i> , <i>Rhizobium tubonense</i> , <i>Rhizobium tibeticum</i> , <i>Rhizobium mesoamericanum</i> CCGE 501, <i>Rhizobium herbae</i> , <i>Rhizobium endophyticum</i>	99.54	Proteobacteria Alphaproteobacteria Rhizobiales
OTU.19	2.44	<i>Rhizobium</i> spp., <i>Arthrobacter</i> spp.	99.54	Proteobacteria Alphaproteobacteria Rhizobiales
OTU.90	2.94	<i>Sphingopyxis panaciterrae</i> , <i>Sphingopyxis chilensis</i> , <i>Sphingopyxis</i> sp. BZ30, <i>Sphingomonas</i> sp.	100.0	Proteobacteria Alphaproteobacteria Sphingomonadales
OTU.518	4.8	<i>Hydrogenophaga intermedia</i>	100.0	Proteobacteria Betaproteobacteria Burkholderiales
OTU.1312	4.07	<i>Paucimonas lemoignei</i>	99.54	Proteobacteria Betaproteobacteria Burkholderiales
OTU.5	3.69	<i>Delftia tsuruhatensis</i> , <i>Delftia lacustris</i>	100.0	Proteobacteria Betaproteobacteria Burkholderiales
OTU.114	2.78	<i>Herbaspirillum</i> sp. SUEMI03, <i>Herbaspirillum</i> sp. SUEMI10, <i>Oxalicibacterium solurbis</i> , <i>Hermiimonas fonticola</i> , <i>Oxalicibacterium horti</i>	100.0	Proteobacteria Betaproteobacteria Burkholderiales
OTU.633	3.84	No hits of at least 90% identity	89.5	Proteobacteria Deltaproteobacteria Myxococcales
OTU.3594	3.83	<i>Chondromyces robustus</i>	90.41	Proteobacteria Deltaproteobacteria Myxococcales
OTU.442	3.05	<i>Chondromyces robustus</i>	92.24	Proteobacteria Deltaproteobacteria Myxococcales
OTU.32	3.0	<i>Sandaracinus amylolyticus</i>	94.98	Proteobacteria Deltaproteobacteria Myxococcales
OTU.228	2.54	<i>Sorangium cellulosum</i>	98.17	Proteobacteria Deltaproteobacteria Myxococcales
OTU.899	2.28	<i>Enhygromyxa salina</i>	97.72	Proteobacteria Deltaproteobacteria Myxococcales
OTU.6	3.62	<i>Cellvibrio fulvus</i>	100.0	Proteobacteria Gammaproteobacteria Pseudomonadales
OTU.11	5.25	<i>Stenotrophomonas pavanii</i> , <i>Stenotrophomonas maltophilia</i> , <i>Pseudomonas geniculata</i>	99.54	Proteobacteria Gammaproteobacteria Xanthomonadales
OTU.6062	4.83	<i>Dokdonella</i> sp. DC-3, <i>Luteibacter rhizovicinus</i>	97.26	Proteobacteria Gammaproteobacteria Xanthomonadales
OTU.154	3.24	<i>Pseudoxanthomonas mexicana</i> , <i>Pseudoxanthomonas japonensis</i>	100.0	Proteobacteria Gammaproteobacteria Xanthomonadales
OTU.100	2.66	<i>Pseudoxanthomonas sacheonensis</i> , <i>Pseudoxanthomonas dokdonensis</i>	100.0	Proteobacteria Gammaproteobacteria Xanthomonadales
OTU.1023	4.61	No hits of at least 90% identity	80.54	Verrucomicrobia Spartobacteria Chthoniobacterales
OTU.266	4.54	No hits of at least 90% identity	83.64	Verrucomicrobia Spartobacteria Chthoniobacterales
OTU.541	4.49	No hits of at least 90% identity	84.23	Verrucomicrobia Spartobacteria Chthoniobacterales
OTU.185	4.37	No hits of at least 90% identity	85.14	Verrucomicrobia Spartobacteria Chthoniobacterales
OTU.2192	3.49	No hits of at least 90% identity	83.56	Verrucomicrobia Spartobacteria Chthoniobacterales
OTU.1533	3.43	No hits of at least 90% identity	82.27	Verrucomicrobia Spartobacteria Chthoniobacterales
OTU.241	3.38	No hits of at least 90% identity	87.73	Verrucomicrobia Spartobacteria Chthoniobacterales
OTU.83	5.61	<i>Luteolibacter</i> sp. CCTCC AB 2010415	97.72	Verrucomicrobia Verrucomicrobiae Verrucomicrobiales
OTU.627	4.43	<i>Verrucomicrobiaceae</i> bacterium DC2a-G7	100.0	Verrucomicrobia Verrucomicrobiae Verrucomicrobiales
OTU.638	4.0	<i>Luteolibacter</i> sp. CCTCC AB 2010415, <i>Luteolibacter algae</i>	93.61	Verrucomicrobia Verrucomicrobiae Verrucomicrobiales

Table 2: <sup>13</sup>C-xylose responders BLAST against Living Tree Project

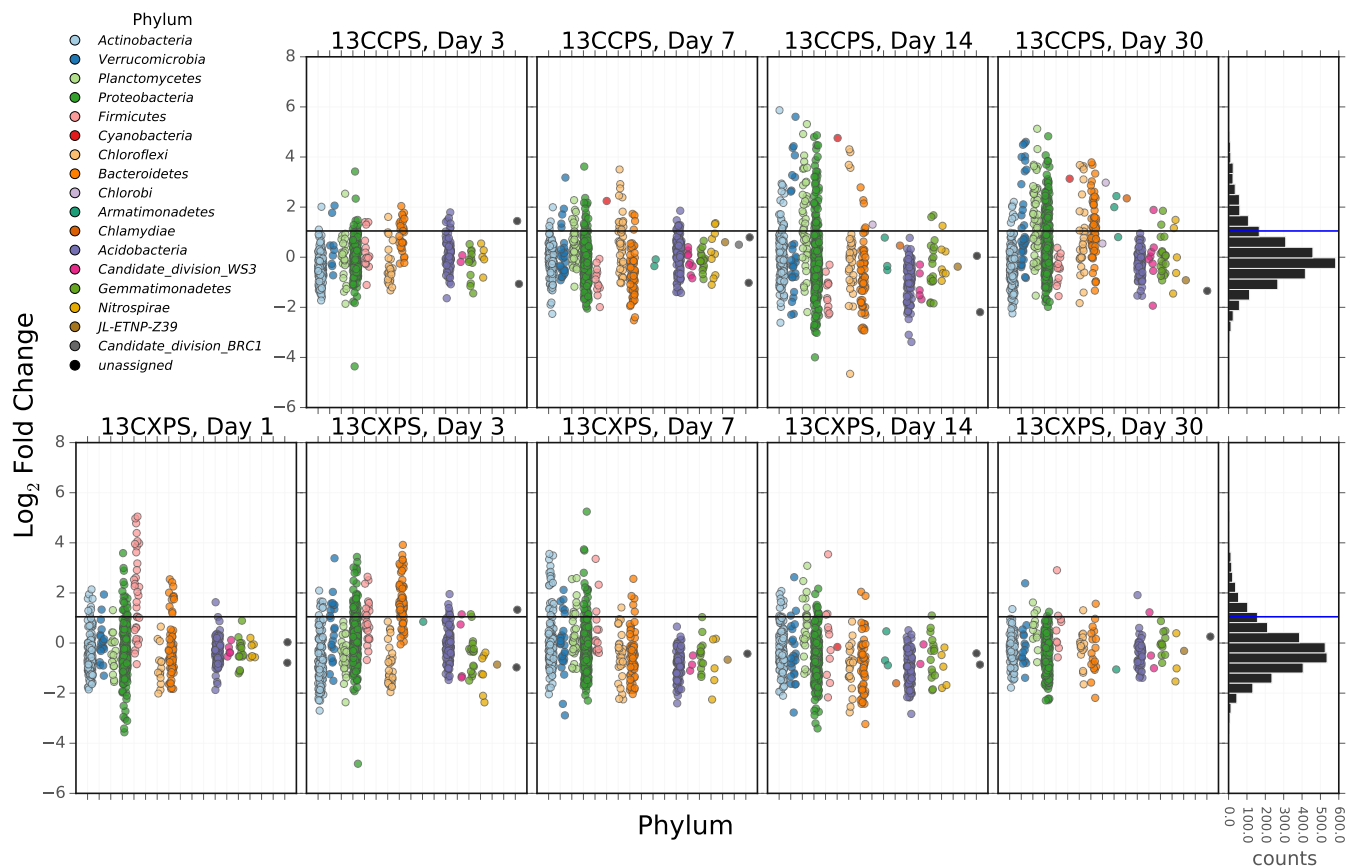
OTU ID	Fold change	Top BLAST hits	BLAST %ID	Phylum;Class;Order
OTU.4446	3.49	<i>Catenuloplanes niger</i> , <i>Catenuloplanes castaneus</i> , <i>Catenuloplanes atrovinosus</i> , <i>Catenuloplanes crispus</i> , <i>Catenuloplanes nepalensis</i> , <i>Catenuloplanes japonicus</i>	97.72	Actinobacteria Frankiales Nakamurellaceae
OTU.62	2.57	<i>Nakamurella flavida</i>	100.0	Actinobacteria Frankiales Nakamurellaceae
OTU.24	2.81	<i>Cellulomonas aerilata</i> , <i>Cellulomonas humilata</i> , <i>Cellulomonas terrae</i> , <i>Cellulomonas soli</i> , <i>Cellulomonas xylanilytica</i>	100.0	Actinobacteria Micrococcales Cellulomonadaceae
OTU.4	2.84	<i>Agromyces ramosus</i>	100.0	Actinobacteria Micrococcales Microbacteriaceae
OTU.37	2.68	<i>Phycicola gilvus</i> , <i>Microterricola viridarii</i> , <i>Frigoribacterium faeni</i> , <i>Frondihabitans sp. RS-15</i> , <i>Frondihabitans australicus</i>	100.0	Actinobacteria Micrococcales Microbacteriaceae
OTU.5284	3.56	<i>Isoptericola nanjingensis</i> , <i>Isoptericola hypogeus</i> , <i>Isoptericola variabilis</i>	98.63	Actinobacteria Micrococcales Promicromonosporaceae
OTU.252	3.34	<i>Promicromonospora thailandica</i>	100.0	Actinobacteria Micrococcales Promicromonosporaceae
OTU.244	3.08	<i>Cellulosimicrobium funkei</i> , <i>Cellulosimicrobium terreum</i>	100.0	Actinobacteria Micrococcales Promicromonosporaceae
OTU.760	2.89	<i>Dyadobacter hamtensis</i>	98.63	Bacteroidetes Cytophagia Cytophagales
OTU.14	3.92	<i>Flavobacterium oncorhynchi</i> , <i>Flavobacterium glycines</i> , <i>Flavobacterium succinicans</i>	99.09	Bacteroidetes Flavobacteria Flavobacteriales
OTU.6203	3.32	<i>Flavobacterium granuli</i> , <i>Flavobacterium glaciei</i>	100.0	Bacteroidetes Flavobacteria Flavobacteriales
OTU.159	3.16	<i>Flavobacterium hibernum</i>	98.17	Bacteroidetes Flavobacteria Flavobacteriales
OTU.2379	3.1	<i>Flavobacterium pectinovorum</i> , <i>Flavobacterium sp. CS100</i>	97.72	Bacteroidetes Flavobacteria Flavobacteriales
OTU.131	3.07	<i>Flavobacterium fluvii</i> , <i>Flavobacteria bacterium HMD1033</i> , <i>Flavobacterium sp. HMD1001</i>	100.0	Bacteroidetes Flavobacteria Flavobacteriales
OTU.3540	2.52	<i>Flavobacterium terrigena</i>	99.54	Bacteroidetes Flavobacteria Flavobacteriales
OTU.107	2.25	<i>Flavobacterium sp. 15C3</i> , <i>Flavobacterium banpakuense</i>	99.54	Bacteroidetes Flavobacteria Flavobacteriales
OTU.277	3.52	<i>Solibius ginsengiterrae</i>	95.43	Bacteroidetes Sphingobacteriia Sphingobacteriales
OTU.183	3.31	No hits of at least 90% identity	89.5	Bacteroidetes Sphingobacteriia Sphingobacteriales
OTU.5906	3.16	<i>Terrimonas sp. M-8</i>	96.8	Bacteroidetes Sphingobacteriia Sphingobacteriales
OTU.360	2.98	<i>Flavisolibacter ginsengisoli</i>	95.0	Bacteroidetes Sphingobacteriia Sphingobacteriales
OTU.369	5.05	<i>Paenibacillus sp. D75</i> , <i>Paenibacillus glycanilyticus</i>	100.0	Firmicutes Bacilli Bacillales
OTU.267	4.97	<i>Paenibacillus pabuli</i> , <i>Paenibacillus tundrae</i> , <i>Paenibacillus taichungensis</i> , <i>Paenibacillus xylanexedens</i> , <i>Paenibacillus xylanilyticus</i>	100.0	Firmicutes Bacilli Bacillales
OTU.1040	4.78	<i>Paenibacillus daejeonensis</i>	100.0	Firmicutes Bacilli Bacillales

Table 2 – continued from previous page

OTU ID	Fold change	Top BLAST hits	BLAST %ID	Phylum;Class;Order
OTU.57	4.39	<i>Paenibacillus castaneae</i>	98.62	Firmicutes Bacilli Bacillales
OTU.394	4.06	<i>Paenibacillus pocheonensis</i>	100.0	Firmicutes Bacilli Bacillales
OTU.319	3.98	<i>Paenibacillus xinjiangensis</i>	97.25	Firmicutes Bacilli Bacillales
OTU.5603	3.96	<i>Paenibacillus uliginis</i>	100.0	Firmicutes Bacilli Bacillales
OTU.1069	3.85	<i>Paenibacillus terrigena</i>	100.0	Firmicutes Bacilli Bacillales
OTU.843	3.62	<i>Paenibacillus agarexedens</i>	100.0	Firmicutes Bacilli Bacillales
OTU.2040	2.91	<i>Paenibacillus pectinilyticus</i>	100.0	Firmicutes Bacilli Bacillales
OTU.3	2.61	[ <i>Brevibacterium</i> ] <i>frigoritolerans</i> , <i>Bacillus</i> sp. LMG 20238, <i>Bacillus coahuilensis</i> m4-4, <i>Bacillus simplex</i>	100.0	Firmicutes Bacilli Bacillales
OTU.335	2.53	<i>Paenibacillus thailandensis</i>	98.17	Firmicutes Bacilli Bacillales
OTU.3507	2.36	<i>Bacillus</i> spp.	98.63	Firmicutes Bacilli Bacillales
OTU.8	2.26	<i>Bacillus niacini</i>	100.0	Firmicutes Bacilli Bacillales
OTU.4743	2.24	<i>Lysinibacillus fusiformis</i> , <i>Lysinibacillus sphaericus</i>	99.09	Firmicutes Bacilli Bacillales
OTU.9	2.04	<i>Bacillus megaterium</i> , <i>Bacillus flexus</i>	100.0	Firmicutes Bacilli Bacillales
OTU.22	2.8	<i>Paracoccus</i> sp. NB88	99.09	Proteobacteria Alphaproteobacteria Rhodobacterales
OTU.346	3.44	<i>Pseudoduganella violaceinigra</i>	99.54	Proteobacteria Betaproteobacteria Burkholderiales
OTU.68	3.74	<i>Shigella flexneri</i> , <i>Escherichia fergusonii</i> , <i>Escherichia coli</i> , <i>Shigella sonnei</i>	100.0	Proteobacteria Gammaproteobacteria Enterobacteriales
OTU.290	3.59	<i>Pantoea</i> spp., <i>Kluyvera</i> spp., <i>Klebsiella</i> spp., <i>Erwinia</i> spp., <i>Enterobacter</i> spp., <i>Buttiauxella</i> spp.	100.0	Proteobacteria Gammaproteobacteria Enterobacteriales
OTU.48	2.99	<i>Aeromonas</i> spp.	100.0	Proteobacteria Gammaproteobacteria aaa34a10



**Fig. 1.** NMDS analysis from weighted unifrac distances of 454 sequence data from SIP fractions of each treatment over time. Twenty fractions from a CsCl gradient fractionation for each treatment at each time point were sequenced (Fig. S1). Each point on the NMDS represents the bacterial composition based on 16S sequencing for a single fraction where the size of the point is representative of the density of that fraction and the colors represent the treatments (A) or days (B).



**Fig. 2.** Log<sub>2</sub> fold change of <sup>13</sup>C-responders in cellulose treatment (top) and xylose treatment (bottom). Log<sub>2</sub> fold change is based on the relative abundance in the experimental treatment compared to the control within the density range 1.7125-1.755 g ml<sup>-1</sup>. Taxa are colored by phylum. ‘Counts’ is a histogram of number of sequences for each log<sub>2</sub> fold change value.

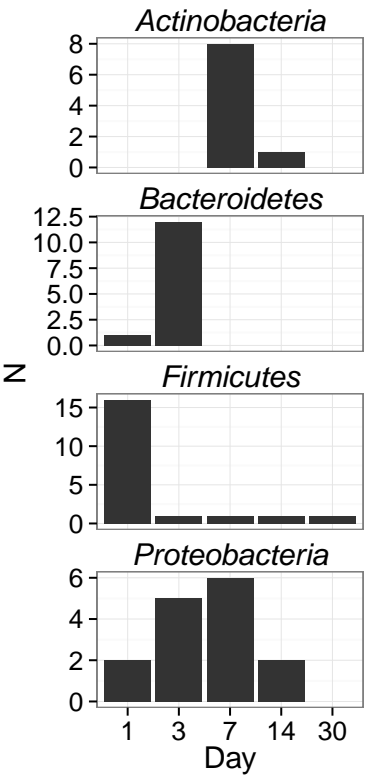


**Fig. 3.** Counts of  $^{13}\text{C}$ -xylose responders in the *Actinobacteria*, *Bacteroidetes*, *Firmicutes* and *Proteobacteria* at days 1, 3, 7 and 30.

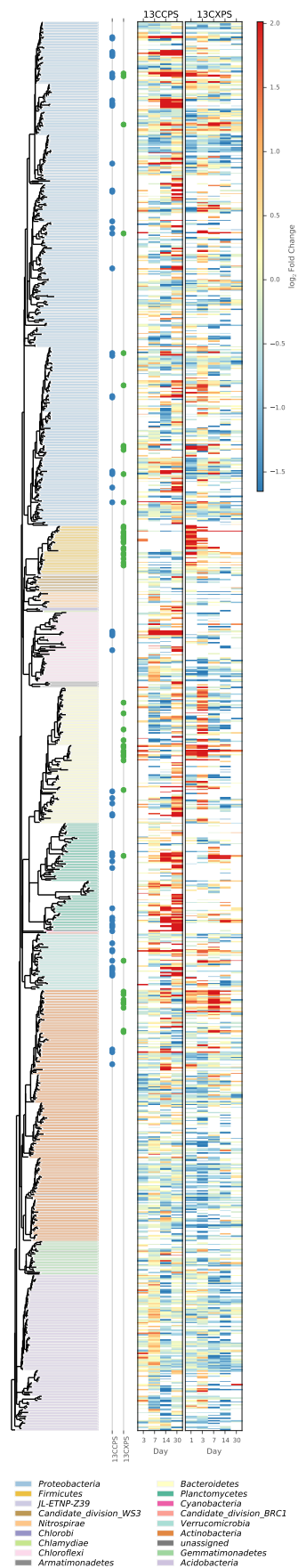


**Fig. 4.** Phylogenetic tree of sequences passing a user defined sparsity threshold (0.6) for at least one day of the time series. Branches are colored by phylum. <sup>13</sup>C-responders for cellulose (blue) and xylose (green) are indicated by a point beside the respective branch. Heatmap demonstrates log<sub>2</sub> fold change of each taxa through the full time series for both treatments (cellulose, left; xylose, right).

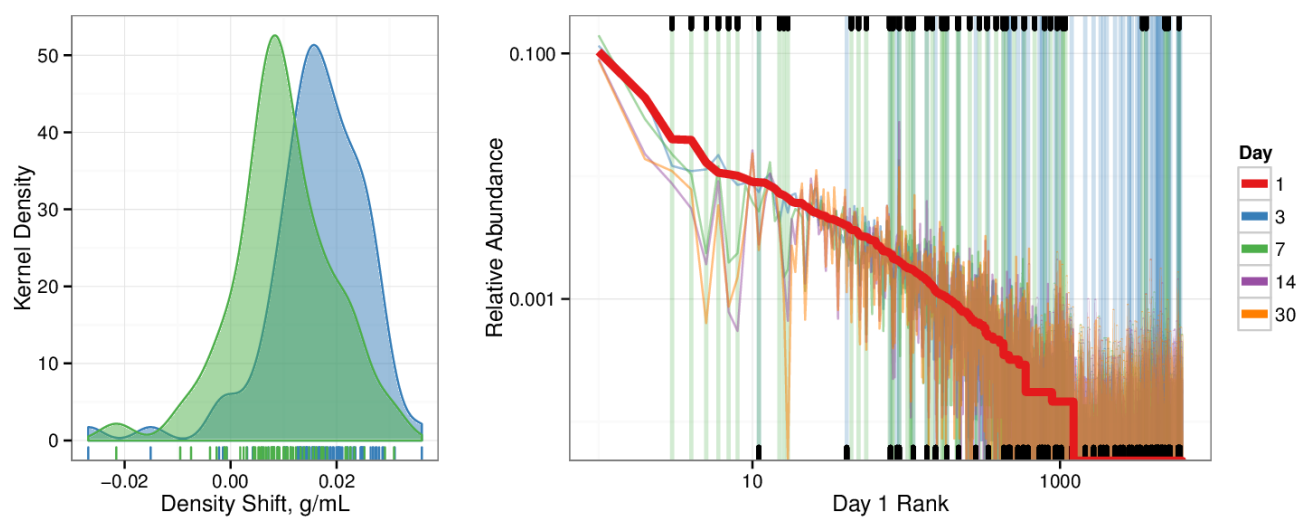


**Fig. 5.**  $^{13}\text{C}$ -responder characteristics based on density shift (A) and rank (B). Kernel density estimation of  $^{13}\text{C}$ -responder's density shift in cellulose treatment (blue) and xylose treatment (green) demonstrates degree of labeling for responders for each respective substrate.  $^{13}\text{C}$ -responders in rank abundance are labeled by substrate (cellulose, blue; xylose, green). Ticks at top indicate location of  $^{13}\text{C}$ -xylose responders in bulk community. Ticks at bottom indicate location of  $^{13}\text{C}$ -cellulose responders in bulk community. OTU rank was assessed from day 1 bulk samples.

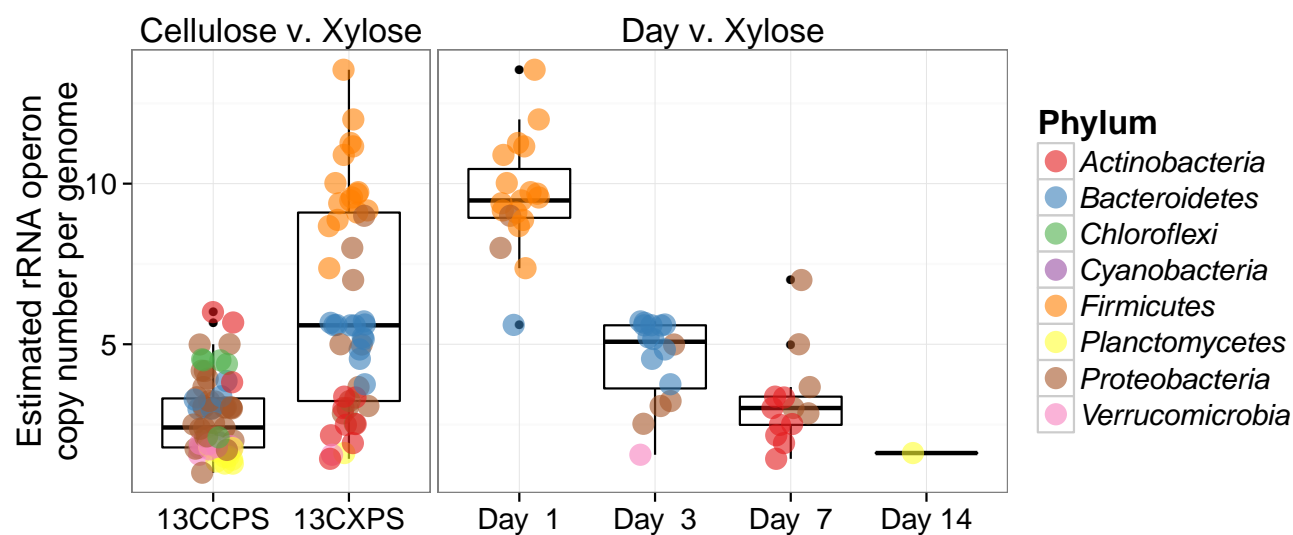


**Fig. 6.** Estimated rRNA operon copy number per genome for  $^{13}\text{C}$  responding OTUS. Panel titles indicate which labeled substrate(s) are depicted.

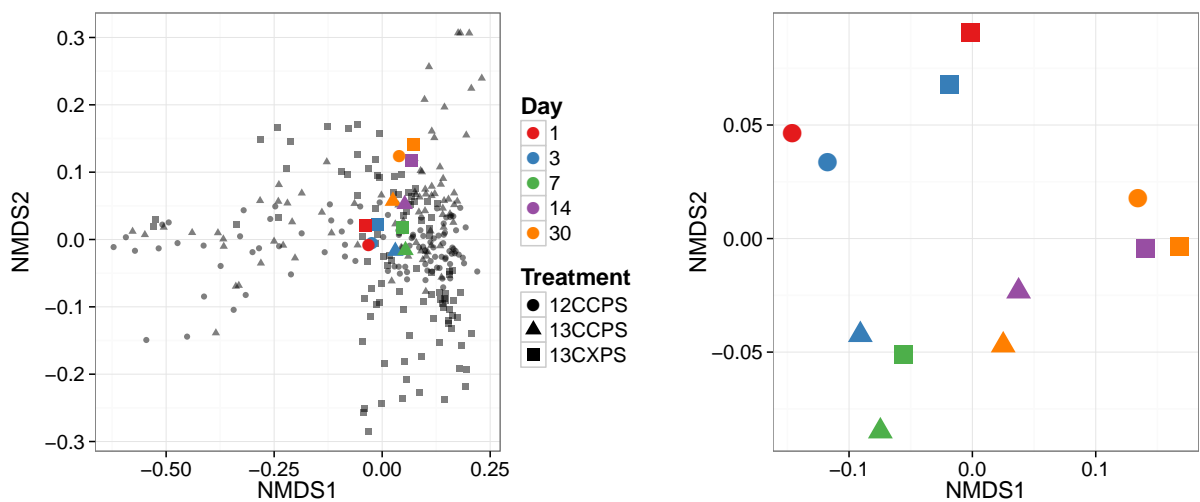


Fig. 7. Ordination of bulk gradient fraction phylogenetic profiles.

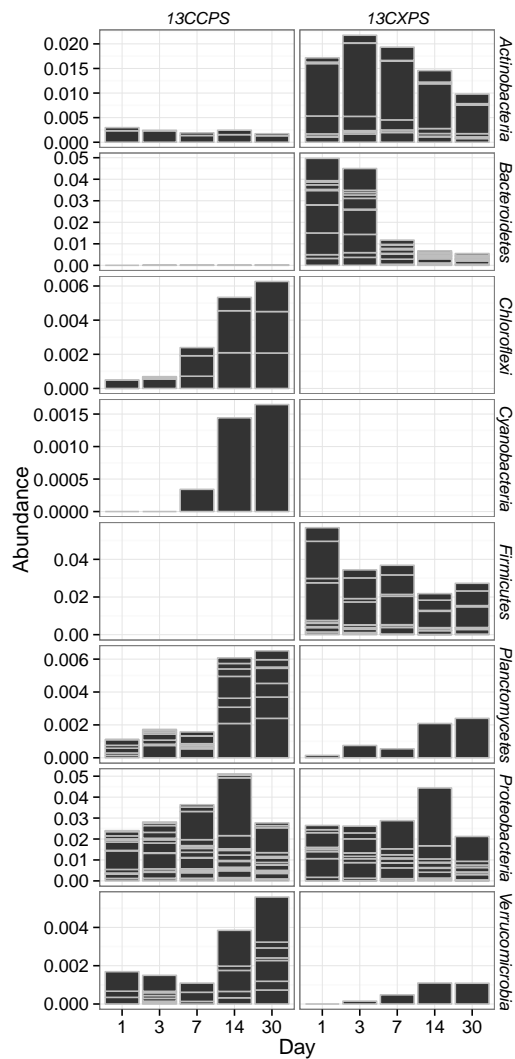
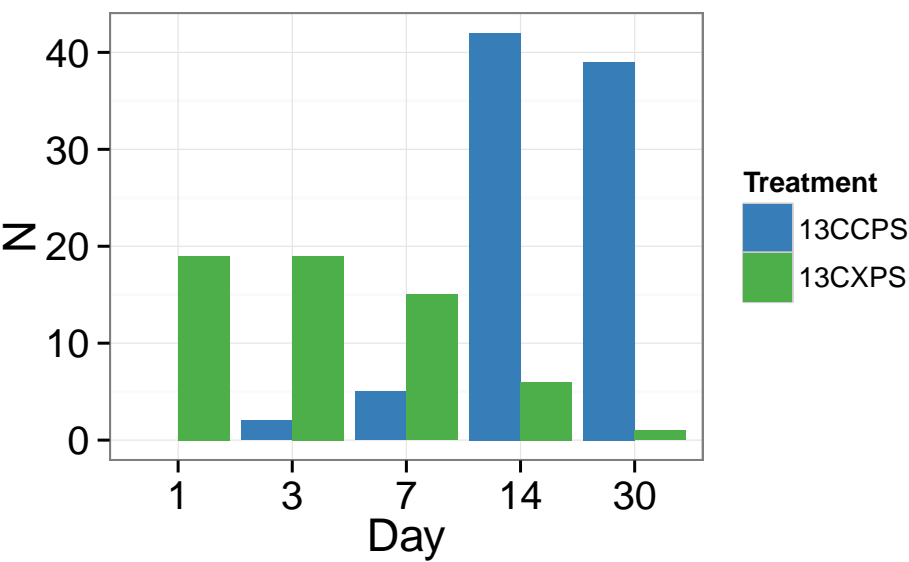


Fig. 8. Sum of bulk abundances with each phylum for responder OTUs.





**Fig. 9.** Counts of responders to each isotopically labeled substrate (cellulose and xylose) over time.